Journal Name

ARTICLE

Hydrated Polysaccharide Multilayer as Intraocular Lens Surface Coating for Biocompatibility Improvement

Quankui Lin,[*a] Xu Xu,[a] Bailiang Wang,[a] Chenghui Shen,[b] Junmei Tang, [a] Yuemei Han,[a] and Hao Chen[*a]

Posterior capsule opacification (PCO) is a significant complication of intraocular lens (IOL) implantation in cataract surgery, in which the adhesion and proliferation of lens epithelial cells (LEC) on the IOL surface play important roles. In present study, highly swollen hyaluronic acid (HA)/chitosan (CHI) polyelectrolyte multilayer was fabricated on IOL surface via layer by layer technique. Quartz crystal microbalance with dissipation (QCM-D) result not only shows the successful construction of the multilayer, but also indicates its hydrogel-like swollen property. The water content of the $(HA/CHI)_5$ multilayer is around 400%, obtained by Thermogravimetry (TG) analysis. Compared with pristine IOL, the polysaccharide multilayer modification doesn't influence its optical property, whereas the adhesion and proliferation of LEC are greatly inhibited. In vivo ocular implantation results show that such polysaccharide multilayer modification presents good in vivo biocompatibility, and have positive effects on reducing the PCO development.

Introduction

Cataract is a common eye disease and causes millions of blind in the world. The most effective clinical surgeries are phacoemulsification with intraocular lens (IOL) implantation, on account of its small incision, quick recovery and better postoperative vision.[1] However, posterior capsule opacification (PCO), which is the most common complication and causes decrease of vision months to years after cataract surgery, greatly affects the curability of cataract.[2] PCO is regarded to be the result of the adhesion and proliferation of the residual lens epithelial cells (LEC) onto the implanted IOL after cataract surgery,[3] as wound healing promotes residual LEC to proliferate, differentiate, and to deposit extracellular matrix, via autocrine and paracrine cell signaling.[4] Although PCO has been extensively investigated, there is no established mechanism to explain the cause.[5] Most current studies hypothesize that a multicellular secondary membrane results from migration and fibrosis of residual LEC on the posterior capsule, forming Soemmerring ring (elschnig pearls).[6] Others suggest that a single layer of residual anterior capsule epithelial cells migrate onto the posterior capsule and undergo metaplasia into myofibroblasts, pulling the posterior capsule into many tiny folds.[7] Both mechanisms can contribute to the development of PCO.[2, 5-8]

Several reports have focused on how to prevent PCO in the past decades. In addition to the progress of the operation technique and the position of capsulorhexis, IOL materials are important factors in the development of PCO.[9-12] The effect of IOL on PCO has been explained by various suppositions such as the separation of the posterior capsule from the anterior capsule, stretching of the capsule, compression, no space/no cells and adhesiveness of the IOL material.[2, 5, 6, 9] Among various commercial IOL, silicone intraocular lens, due to their advantages of high transmittance, relatively inert, flexibility, and suitable refractive index, has been frequently used soft IOL.[13] On the other hand, it has been found that the surface of silicone IOL is easy to adhere bacteria and cells, which may cause high incidence of endophthalmitis or PCO.[14] This disadvantage cause lots of inconvenience to the patients and greatly limits its application. IOL materials design to control the LEC adhesion and proliferation provides a possible approach to prevent PCO.[6, 15-17] Several attempts have been explored to improve the biocompatibility of IOL materials in the past decades. Such as surface immobilization of heparin, titanium coating, Teflon-coating, surface PEG or phospholipid moieties tethering.[10-12, 14, 18-23] Such surface modification procedures have significantly improved the biocompatibility of the IOL. The LEC adhesion or proliferation was decreased after surface modifications.[10, 11, 20-23] However, most of these approaches require relatively complicate chemical grafting process or involve organic solvent to ensure the immobilization of the surface coatings, which may be an underlying element of visual acuity decrease.[24] The mild IOL surface modification strategies are on the earth.

Surface modification of biomaterials with polyelectrolyte multilayer (PEM) to obtain biocompatible coatings via layer by layer (LbL) technique has gained more and more attention in recent decades.[25-27] With advantages of the possibility in maintaining the biomacromolecular activity and the flexibility to the complicated fabric matrix, PEM has been applied to implantable biomaterials modification for improved

cytocompatiblity and hemocompatibility.[28-33] Besides improved cell adhesion and proliferation, PEM with cell-resistant property can be obtained via controlling the fabrication conditions.[34-36] Herein, PEM with hyaluronic acid (HA) and chitosan (CHI) as components was constructed and used to IOL surface modification. Taking advantages of the hydrated property of the polysaccharides, the aim of this work was to generate a hydrogel-like coating on IOL surface, thus inhibit the LEC adhesion and proliferation, aiming to prevent PCO occurrence.

Materials and methods

Materials

HA was purchased from Freda Biochem Co., Ltd. CHI, with 92% degree of deacetylation and molecular weight around 300 kDa, was supplied by Sangon Biotech Co., Ltd. Branched polyethylenimine (PEI), fluorescein diacetate (FDA) were provided by Sigma-Aldrich. bicinchoninic acid (BCA) kits is obtained from Beyotime Biotechnol Co., Ltd.. Masson trichrome is purchased from Leagene Biotechnol Co., Ltd. Polydimethylsiloxane (PDMS) was prepared from Sylgard® 184 from Dow Corning, according to the manufacturer's instructions, using 10:1 ratio of elastomer base to curing agent. Foldable intraocular lens for animal experiments uses were purchased from ExLen® Medical (Diameter of silicone biconvex optic: 6 mm, PMMA modified C design haptics) or Alcon® (research use only, not for clinical use). Human lens epithelial cell line was provided by ATCC (HLE B3, CRL-11421™). All other chemicals were of analytical grade and used without further purification.

PEM fabrication

The PDMS silicone materials or IOL were used as the substrate for PEM fabrication. The fabrication procedure was the same as our previous publications.[30, 32-34] Each experiment was initiated by PEI adsorption for 1 hr, which resulted in a stable positively charged substrate surface. Then the substrates were dipped in 1mg/mL HA solution for 15 min and followed with acetic buffer solution rinsing. The HA adsorbed substrates were then dipped into 1mg/mL CHI solution for 15 min and followed with the same rinsing process as before. The alternate polyelectrolyte deposition circle was continued until determined bilayers of (HA/CHI) were obtained.

The multilayer growth was followed by quartz crystal microbalance (QCM) measurements. QCM measurements were carried out on quartz crystal microbalance with dissipation (QCM-D, Q-sense AB, Sweden).[30] The quartz crystal was excited at its fundamental frequency (~5 MHz, v=1), as well as at the 3rd, 5th, 7th, 9th and 11th overtones (v=3, 5, 7, 9, 11 corresponding to 15, 25, 35, 45, 55 MHz, respectively). Changes in resonance frequencies (ΔF) and in relaxation (ΔD) of the vibration once the excitation is stopped were recorded. In detail, the clean quartz crystal was settled in the QCM chamber and the acetic buffer was injected for equilibrium. Then the PEI solution was injected at 100 μL/min continuously until the QCM traces did not vary, followed by the buffer pump in the same speed. Then the HA solution was injected in the same speed until equilibrium and followed the same buffer injection. After that the CHI solution was injected in the same speed until equilibrium and followed the same buffer injection. HA and CHI were then alternately injected into the chamber for buildup multilayers. The curves of frequency shift vs. time and

dissipation vs. time were recorded respectively. The hydrated multilayer thicknesses were modeled and analyzed by using the Qtools software (QTools 401) provided with the instrument. The growth of (HA/CHI) multilayer was also followed by spectroscopic ellipsometry (M-2000DI™ ellipsometer, J.A.Woollam. Co., Inc.), equipped with an EC-400 electronics control module and QTH light source. In brief, HA/CHI multilayer was fabricated on Si/SiO₂ wafer, using aforementioned dip coating method except that the multilayer was allowed to dry by nitrogen stream after each buffer rinsing. The dry thicknesses of the multilayer were obtained from the software of the instrument.

PEM physical and optical property investigation

The surface topography of (HA/CHI) PEM in different bilayers was obtained via atomic force microscopy (AFM) by tapping mode. The water content of the multilayer was determined via thermogravimeric analysis (TGA). The polysaccharide multilayer modified IOL were observed via fluorescent microscopy. The transmittance of the modified IOL was investigated by UV-Vis spectroscopy. For TGA test, the multilayers were fabricated on silicone as aforementioned. Then the multilayer films were scraped and weighted for TGA investigation. The heating rate is 10 ℃/min, and maintained at 100 ℃ for 5 min. The heating process was finished when the temperature at 800 ℃.

Protein Adsorption

Bovine serum albumin (BSA) was used as a model protein to test the protein adsorption on the multilayer modified IOL material surface. The protein adsorption was obtained via BCA kits. After being equilibrated with PBS overnight in 96 well plate, the HA/CHI multilayer coated silicone substrates were immersed in 0.2 mL of BSA at 37 ℃ for 90 min and then rinsed with PBS three times. The adsorbed proteins were determined using the BCA method at 570 nm. Independent measurements were taken from triplicate samples and the relatively adsorbed protein ratios were calculated with the pristine silicone IOL material as control.

LEC adhesion and proliferation assessment

Lens epithelial cell line (LEC) derived from human lens was cultured and used to assess the cell response to the materials. After confluence, the cells were detached by 0.25% trypsin. The detached cells were resuspended in RPMI-1640 medium and distributed onto 24-well plates containing the multilayer-coated materials (1.5×10^4 cells per well). The cell adhesion was tested at 4 h. The medium were renewed every two days. The cells at 3 days were investigated for proliferation evaluation. At the setting time point, the cells were stained by FDA and visualized by fluorescent microscopy (Zeiss, Germany). Fluorescent images were acquired at 20 × objective in fluorescein filter (488 nm/excitation). The behaviors of LEC on the polysaccharide multilayer modified IOL material were evaluated subsequently. The cell initial adhesion and proliferation were measured. The cell distribution was assessed as well.

In vivo intraocular implantation and evaluation

The approval of the local laboratory animal committee (Laboratory Animal Ethics Committee of Wenzhou Medical University) for this study was obtained. Experiments were carried out in New Zealand White rabbits, weighing between 2.5 and 3.5 kg (obtained from Animal Administration Center of Wenzhou Medical University). The rabbits were treated in accordance with guidelines set forth by the Association for Research in Vision and Ophthalmology. Their eyes were grossly checked and found to be unremarkable before the surgical procedures. Phacoemulsification followed by Lens suction was carried on the left eye of each rabbit. Polishing of the cortex was abolished for easy establishing of PCO model. The (HA/CHI)$_5$ multilayer modified IOL was then implanted. The pristine IOL was served as control. All surgeries were performed by the same surgeon (Dr. Xu X). Postoperative topical therapy included combination Levofloxacin eye drops and Tobramycin–dexamethasone ointment during the first postoperative week and prednisolone acetate drops, which were tapered during the first and second postoperative weeks.

The eyes were dilated and evaluated by slit lamp microscopy examination for acute ocular inflammatory response on Day 1, Day 3 and Day 7, postoperatively. No sedation or anaesthesia was used. Clinical color photographs at each time point were obtained with a digital camera attached to the slit lamp microscopy. After one month, the animals were anesthetized and then killed humanely with air embolism. The eyes were enucleated and placed in 10% neutral buffered formalin for at least 24 hours. For histology, tissue was embedded in paraffin and sectioning was performed. The section slides were stained with Masson trichrome, and examined by microscope. For Miyake-Apple view examination, the globes were then bisected coronally just anterior to the equator. Gross examination and photographs from the posterior aspect were performed to assess the PCO development as well as IOL fixation. The severity of PCO was evaluated by estimating the cleanliness of each four quadrants of the entire posterior capsule area within the IOL optic as the reference.[37] In details, 0 (none), 1 (slight, iris pattern still detectable), 2 (obvious, iris pattern barely detectable), or 3 (distinct, iris pattern not detectable). All globes were analyzed for the follows: central PCO (CPCO, graded from 0 to 3), which corresponded to the area including the IOL optic within the pupillary area; peripheral PCO (PPCO, graded from 0 to 3), which corresponded to the area including the IOL optic outside the pupillary area; and Soemmerring ring (graded from 0 to 3 in intensity and area), which corresponded to the area outside the IOL optic and inside the capsular bag. All capsular bags were divided into 4 areas. The intensity of each area was graded and the mean of all 4 areas calculated.

Statistical analysis

The results were expressed as a mean standard error of the mean for each sample. Each experiment was repeated independently three times. Two sample t test in origin 8.0 (Microcal, USA) were used to compare data obtained with the different samples under identical treatments. A value of $p < 0.05$ was considered significant.

Results and discussion

Multilayer fabrication and coating onto IOL

HA is one of natural polysaccharides and exits in vitreous body, skin, joint and extracellular matrix.[38] It is a linear polymer of high molecular weight comprising a glucuronic acid (1-β-3) N-acetylglucosamine (1-β-4) disaccharide repeating unit. When in solution, HA is a negative charged polysaccharide and always take on an expanded and highly hydrated coil structure. The hydrated state has a 1000-fold more water than polymer, which plays an important role in the hydrodynamic properties of the extracellular environment. It is thus used clinically as eye drop solutions, viscoelastic fluid in intraocular surgeries and components to accelerate corneal wound healing in ocular surgeries.[38-40] CHI is the deacetylated product of chitin, which is the only cationic natural polysaccharide.[41] With its positive charge and biocompatibility, CHI has been widely used for biomaterials surface modification, especially used as a component in natural polyelectrolyte multilayer coatings.[34, 42-46] In present study, HA and CHI was used as components to fabricate polysaccharide multilayer coatings on IOL, taking advantage of their highly hydrated property of polysaccharides. The deposition process of HA/CHI multilayer was characterized by QCM-D. QCM-D is a versatile and sensitive sensor technique to measure both adsorbed mass and the viscoelastic properties of adsorbed layers of molecules in liquid. The resonance frequency (F) of the crystal depends on the total oscillating mass, including water coupled to the oscillation.[43] The F decreases when a thin film is attached to the sensor crystal.[30] Fig. 1 shows QCM traces of frequencies at the 3rd, 5th, 7th, 9th, and 11th overtones (v), corresponding to 15, 25, 35, 45, and 55 MHz, respectively. The frequency shift (Δf) vs. time curves clearly show a typical LbL buildup process of HA/CHI multilayer. With each solution injection, a frequency shift is observed. The ladder trace of frequency decrease indicates the successful adsorption of HA or CHI molecules onto the substrate alternatively.
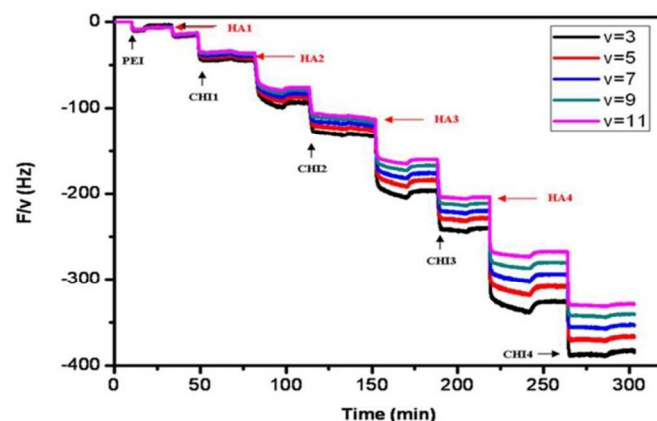

Fig. 1 Frequency shifts in the HA/CHI multilayer deposition under different overtones. The line with the five colors from black to purple represents v =15, 25, 35, 45 and 55 MHz, respectively. The arrows indicate the different polyelectrolytes injection.

Besides multilayer film deposition, ΔF vs. time curves in QCM-D results also show the information of the multilayer hydration state.[43, 47] If the film is thin and rigid, the decrease in frequency is proportional to the mass of the film, and the frequency changes recorded for the fundamental frequency of the crystal superpose with the signals recorded in the higher harmonics. In this way, the QCM operates as a very sensitive balance. However, a film that is "soft" (viscoelastic or swollen) will not fully couple to the oscillation of the crystal. The soft

adhering layer on the crystal leads to the dispersion of the different overtones. The more and more dispersive of the different overtones in the deposition of HA/CHI multilayer indicates the more and more swollen multilayer was obtained with the polysaccharides deposition. The HA/CHI multilayer was introduced onto the IOL surface. The fluorescein isothiocyanate labeled chitosan (CHI^{FITC}) was used instead of chitosan for easy visualization purpose when taking fluorescent photographs. As shown in Fig. 2, LbL technique presents excellent feasibility to fabricate a homogenous thin coating onto the sophisticated 3-D implants. The insertion image shows the optical images of the foldable silicone IOL with two PMMA haptics. It is circular in shape with raised centers, 6 mm in diameter of silicone biconvex optic. The full coverage of the green fluorescence in the surface not only indicates the successful immobilization of the FITC labeled chitosan but also reveals the feasibility of the multilayer coating onto the IOL via regular LbL technique.
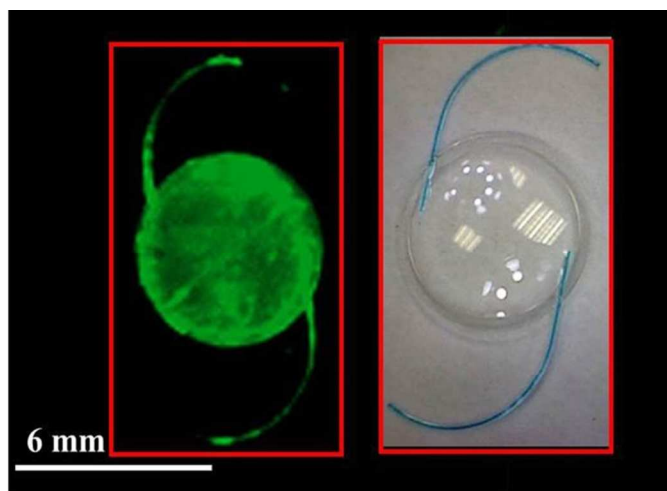

Fig. 2 Fluorescent microscopic image of the (CHI^{FITC}/HA)$_5$ multilayer on IOL. The insertion is the optical image of IOL.

Fig. 3 shows the surface topography of the pristine and HA/CHI multilayer modified silicone materials, observed by AFM. The pristine surface is extremely smooth. The average height of irregularity is 1.7 nm in 5 μm^2 observation area. The introduction of HA and CHI onto the surface induces the increase of roughness. Lots of small particles, islets as nominated,[44, 48] are found in the early stages of the deposition. The average height of irregularity is 6.5 nm after 1 bilayer CHI and HA was deposition and it increases to 55.5 nm after 3 bilayer deposition. The surfaces are fully coated when the multilayer grows further, and no obvious ambits of the islands are found in 5 bilayers. The average height of irregularity decreases to 2.4 nm when (HA/CHI)$_5$ multilayer was fabricated. A similar phenomenon has been reported in the LbL assembly process between polysaccharides.[48] These photographs not only support the successful fabrication of HA/CHI multilayers, but also show that a homogenous surface has been gained when the bilayer number is 5. Fig. 4 shows the light transmittance of the IOL before and after (HA/CHI)$_5$ multilayer modification. The transmittance of pristine silicone IOL material is more than 90% in the visible area. The (HA/CHI)$_5$ multilayer modification doesn't decrease the transmittance significantly. The transmittance of the multilayer modified IOL is also above 90%. This result indicates that the multilayer modification doesn't influents the optical property of IOL, which is of great importance in its actual application.
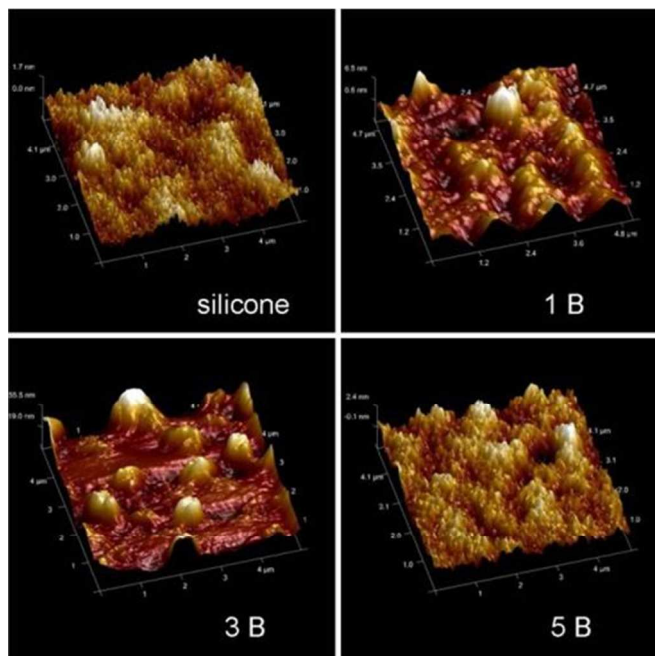

Fig. 3 AFM topographical images of the surface of the silicone substrate, and after the (HA/CHI)$_1$, (HA/CHI)$_3$, or (HA/CHI)$_5$ multilayer modification.
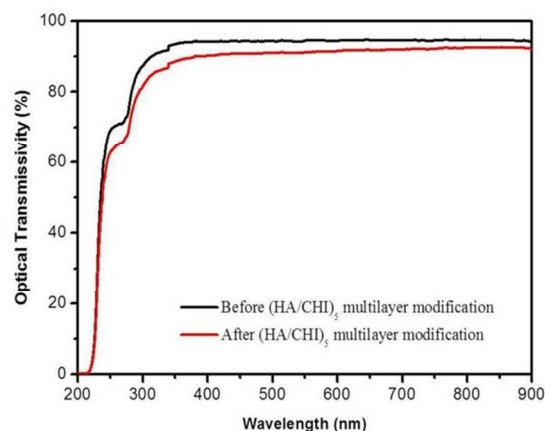

Fig. 4 Optical transmittance of the pristine silicone IOL materials and after (HA/CHI)$_5$ multilayer modification.

Polysaccharide Multilayer structure analysis

As mentioned above, the QCM-D measurement not only demonstrates the HA/CHI multilayer growth, but also provides information about the inner physical structure of the multilayer.[47] As shown in ΔF vs. time curves in Fig. 1, the curves do not superimpose in the different overtones, which indicates that soft multilayer is obtained. Furthermore, the dispersion between the different overtones becomes larger with the multilayer growth. The increasing dispersion indicates that the HA/CHI multilayer grows more and more hydrogel-like swollen.[33] This is also confirmed by the D value analysis in QCM-D measurement. Fig. 5 shows the details of the changes of the D value shift (ΔD) in the deposition circles at overtone of 3, 5, 7, 9 and 11. The ΔD exhibits a sharp increasing trend with the layer number increasing. This result also indicates a more and more swollen multilayer was obtained. The multilayer thicknesses in both dry and hydrated state were thus evaluated

to determine the swollen state by ellipsometry measurement and QCM-D thickness analysis. As shown in Fig. 7, a slow increase of the ellipsometric thickness (circle line) is found in the dried HA/CHI multilayer, whereas a relatively fast increase of QCM-D thickness is observed (square line). The multilayer thickness is at the nanoscale. The differential between QCM-D thickness and ellipsometric thickness becomes larger with the multilayer increase. This confirms that the multilayer becomes more and more hydrated and swollen[43].

TGA was further carried out to quantify the water content in the HA/CHI multilayer. Fig. 7 (a) shows the representative TG for samples loaded with scraped HA/CHI multilayers with different bilayer numbers. The weight loses dramatically with the temperature increasing when below 100 ℃, which is due to the evaporation of the absorbed water when the samples heated. Sustained removal of water of crystallization occurs at the temperature between 100 ℃ and 180 ℃, which shows very slow decrease of the weight loss in the TG curves. A moderate weight loss was occurred after 180 ℃, which was attributed to the decomposition of the polysaccharides. The decomposition was completed at about 500 ℃. There is no significant weight loss over 600 ℃. The HA/CHI multilayer films with different bilayer numbers show the same thermogravimetric behaviors. The remained weight ratios of different multilayer films were calculated and converted to water content in the multilayer was also calculated, the results were shown in Fig. 7 (b). As the solid circle icon shown in Fig. 7(b), all of the remained weight ratios of the HA/CHI multilayers with different bilayer numbers were relatively low. And it decreases with multilayer growth, from 28.8% of $(HA/CHI)_3$ to 18.8% of $(HA/CHI)_{11}$. The converted water contents of HA/CHI multilayers with 3, 5, 7, 9, 11 bilayers were 246.8%, 377.1%, 422.3%, 489.4% and 572.4%, respectively. It is reported that polysaccharides always take on an expanded and highly hydrated coil structure when in the solution, of which HA is most hydrated. The hydrated state of HA has a 1000-fold more water than polymer, which plays an important role in the hydrodynamic properties of the extracellular environment. It is thus used clinically as eye drop solutions, viscoelastic fluid in intraocular surgeries and components to accelerate corneal wound healing in ocular surgeries.[38] Herein, polysaccharide HA and CHI were used as components to fabricated polysaccharides multilayer for IOL materials coating. The QCM-D and TGA results show that the constructed HA/CHI multilayers were swollen and highly hydrated, which may have great effect on reducing the adhesion and proliferation of residue LEC after IOL implantation.
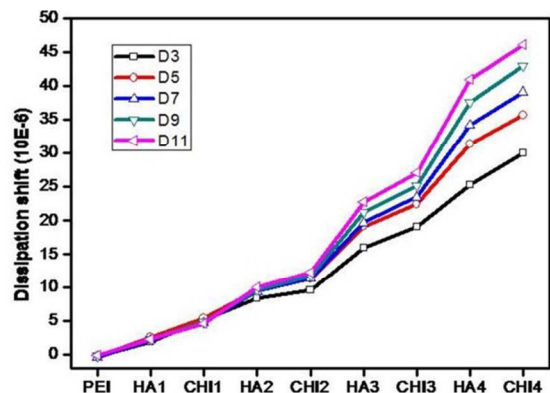

Fig. 5 Dissipation shift (ΔD) of HA/CHI multilayer as a function of layer number in the overtone of 3, 5, 7, 9, and 11.
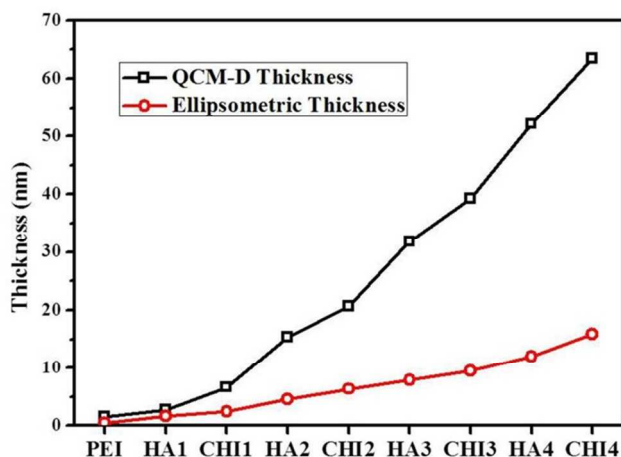

Fig. 6 The multilayer thicknesses increase with the layer number deposition in the fabrication of the HA/chitosan multilayer. The line with square symbols indicates the hydrated thickness obtained from QCM-D analysis and the line with circle symbols indicates the dried thickness obtained from ellipsometry.
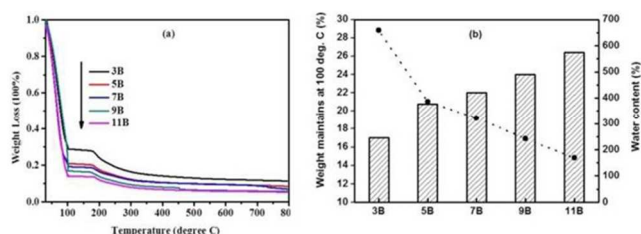

Fig. 7 TG analysis of HA/CHI multilayer with different bilayer numbers. a: The weight loss curve with the temperature. b: The calculated weight maintains at 100 ℃ (solid circle) and the calculated water content of different bilayer number of HA/CHI multilayers (histogram).

In vitro response of protein adsorption and LEC behavior

Protein adsorption onto the foreign implant surface is the first host reaction in the implantation of medical devices. Accordingly, proteins, such as fibronectin, laminin, and collagen have been demonstrated on the surface of implanted IOL.[49] The adsorption of the protein may result in the subsequent cell adhesion and proliferation. In this study, protein adsorption properties of the IOL materials with different HA/CHI multilayers coating was investigated. Fig. 8 shows the results of protein adsorption tests. It can be clearly seen that the adsorbed proteins noticeably increased after PEI pre-coating. As a cationic polyelectrolyte, the coating of PEI on IOL material surface results in the strong positive charged surface, thus increases protein adsorption. Upon deposition of swollen HA/CHI multilayer on the surface, the adsorbed proteins reduced. The relative protein adsorption is around 80% of the unmodified silicone IOL materials. The increasing of the bilayer number does not effect on the protein adsorption, which may be the result of the cationic property of the outmost CHI layer.
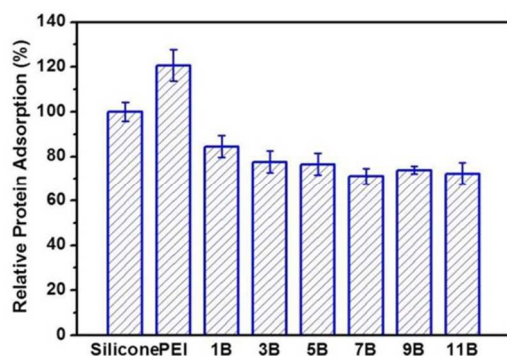
Fig. 8 Protein adsorption on the silicone IOL material surfaces with or without HA/CHI multilayer coatings. 1B, 3B, 5B, 7B, 9B, and 11B refer to 1, 3, 5, 7, 9, 11 Bilayer of HA/CHI multilayer, respectively.

The in vitro LEC adhesion investigation was then carried out. The human lens epithelial cell line was used as models to evaluate the cell effect of the HA/CHI modified silicone IOL materials. The adhesion of the LEC on the IOL is the leading cause of PCO, which results in the second vision lose. As shown in Fig. 9, the initial LEC adhesion onto the pristine silicone IOL materials is 256.3±28.5 cells/mm^2, which is at high cell adhesion level. The same as the protein adsorption, the introduction of the PEI pre-coating increase the LEC adhesion. The adherent cell density increases to 304.3±12.9 cells/mm^2, which is also due to the positive charge of PEI. However, the subsequent HA/CHI multilayer deposition decrease the LEC adhesion. After (HA/CHI)$_1$ deposition, the adherent cell density decrease to 247.4±30.6 cells/mm^2, which is lower than that on pristine materials. The LEC adhesion significantly reduced with an increase of the bilayer number of the polysaccharide multilayers. The adherent cell density decrease to 134.6±27.7 cells/mm^2 after (HA/CHI)$_3$ multilayer modification, and it decrease to 1.2±12.6 cells/mm^2 and 0.7±8.2 cells/mm^2 after 5 and 7 bilayer of (HA/CHI) multilayer deposition. Fig. 10 and Fig. 11 show the representative fluorescent images of LEC adhesion and proliferation on the silicone IOL material surfaces with or without coating of HA/CHI multilayer with different bilayer numbers.

Cells adhered and proliferated well on native (HA/CHI)$_1$ multilayer compared with control surfaces. However, increasing the number of bilayers, thus increasing multilayer thickness caused a significant decrease in LEC adhesion. The initial LEC adhesion is moderate on (HA/CHI)$_3$ multilayer surface, while it is unwilling for the cell proliferation. Seldom LEC can be detected after 3 days culture. Seldom cell can be detected after (HA/CHI)$_5$ multilayer coating, not only at the short adhesion time, but also at the long proliferation times. It can be validated that the (HA/CHI)$_5$ multilayer and (HA/CHI)$_7$ multilayer present excellent property of LEC resistant. These results show that the polysaccharide multilayer modified surfaces greatly reduced LEC initial adhesion and proliferation on the IOL material surface. Up to now, the reported cell resistant multilayers are all polysaccharide-based.[34, 43, 50-52] The highly hydrated polysaccharides make the multilayers swollen and soft, which is proved to be the origin of the cell resistant property. The swollen property and the highly hydrated state of the HA/CHI multilayer were confirmed in this study. The excellent LEC resistant property can be attributed to the highly hydrated state of the polysaccharides multilayer. As indicated by our QCM-D results, in addition to the work of others and our previous, HA/CHI multilayer are soft and viscoelastic,

consistent with a "hydrogel" character that is directly related to the swelling and hydrating properties of these films, suggesting that the observed poor cell adhesion is a result of the cells "regarding" the surface as water, a concept previously suggested by Mendelsohn et al.[54] As the adhesion and proliferation of the LEC on the surface of IOL is the leading cause of PCO, the reduction of LEC adhesion on IOL can restrain the formation of multicellular secondary membrane resulting from migration and fibrosis of residual LEC on the posterior capsule and eventually reduce the incidence of PCO.[5]
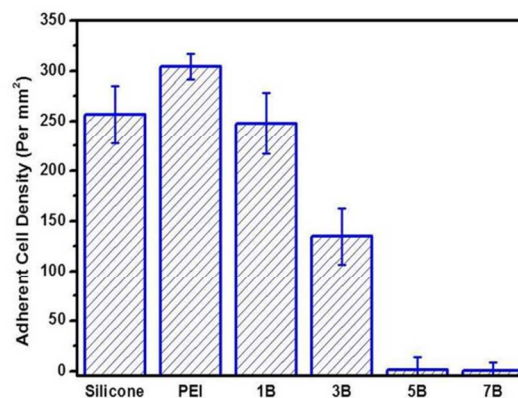

Fig. 9 Adherent lens epithelial cell density on the silicone IOL material surfaces with or without HA/CHI multilayer coatings. 1B, 3B, 5B, and 7B refer to 1, 3, 5, 7 Bilayer of HA/CHI multilayer, respectively.
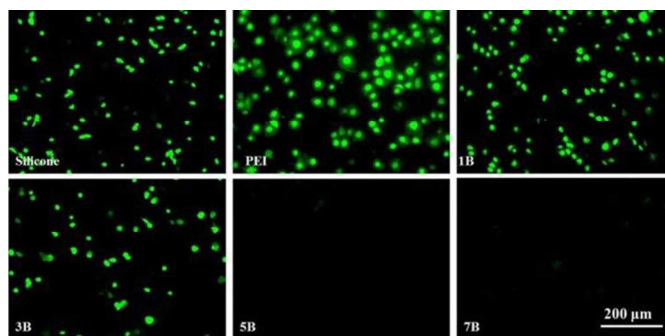

Fig. 10 Representative fluorescent images of lens epithelial cell adhesion on the silicone IOL material surfaces with or without HA/CHI multilayer coatings (4 hours). 1B, 3B, 5B, and 7B refer to 1, 3, 5, 7 Bilayer of HA/CHI multilayer, respectively.
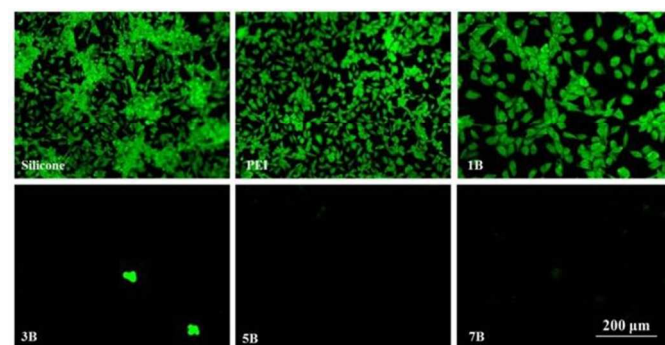

Fig. 11 Representative fluorescent images of lens epithelial cell proliferation on the silicone IOL material surfaces with or without HA/CHI multilayer coatings (3 days). 1B, 3B, 5B, and 7B refer to 1, 3, 5, 7 Bilayer of HA/CHI multilayer, respectively.

In vivo biocompatibility of (HA/CHI)₅ multilayer modified IOL

The (HA/CHI)$_5$ multilayer modified IOL were further implanted in the rabbit eye to evaluate the in vivo response involving both clinical and histological examinations. The pristine IOL were used as controls. There were no cases of postoperative infection and inflammation. As shown in Fig. 12, no anterior chamber exudation or iris synechiae was found in the early periods of postoperative for both control and study groups and no cornea opaque was observed in all cases, indicating that no acute incompatiblity of cornea, iritis, uveitis and vitritis of IOL with or without polysaccharide multilayer modification.

The IOL biocompatibility was further confirmed by histological analysis. The ocular tissues were cross sectioned and examined by microscopy. Cornea is the most sensitive, yet the most important part in the ocular light transmission, with 5 layered structures, including epithelium, Bowman's membrane, stroma, Descemet membrane and endothelium, were visible with normal morphology.[53] Iris is the tissues for blood supply in the eye, with plenty of small blood vessels and folds. As shown in Fig. 13, all tissues, including the cornea and iris were normal in the study groups, which indicate good in vivo biocompatibility of the IOL. However, there was some cortex or residue LEC adhered on the control group whereas the polysaccharide multilayer modified IOL remain clean and clear on the postoperative 7 days. Fig. 14 shows the gross photographs of a rabbit eye in each IOL groups from a posterior Miyake-Apple view. There was some opacity on the peripheral optic of the polysaccharide multilayer modified IOL, whereas obvious opacity on the peripheral and central of the unmodified IOL was observed. Both of the groups developed Soemmerring rings. Fig. 15 shows the PCO and Soemmerring ring scores. The peripheral PCO (PPCO) score in both groups under such experimental condition were high, with no significant difference in the two groups (2.30±0.84 in control group and 1.98±0.70 in multilayer modified IOL group, p>0.05). However, compared with the score of central PCO (CPCO) in control group (2.35±0.19), the CPCO score in multilayer modified group was low (1.23±0.10), the difference was significant (p<0.05). Most eyes developed a high degree of Soemmerring ring (SR), with no statistically significant difference between the two groups.

Recent research have illustrated that the residue LEC or cortex adhesion on the IOL may be the origin of the PCO.[3] The residue LEC are likely to adherent on the hydrophobic IOL materials. Cell migration, proliferation and epithelial-mesenchymal transition of the adherent LEC are followed on the IOL material.[8] Surface modification to reduce the cell adhesion suggests a promising way to improve the surface property of the implantable materials.[3, 4, 6, 7, 10-12, 20] In previous studies, we have fabricated cytocompatible coatings via layer by layer deposition of the natural polyelectrolytes for fast endothelialization of the cardiovascular stents.[30, 32, 33] The endothelial cell selective surface has also been generated onto the stent material surface via the combination of the resistant natural polyelectrolyte multilayer and the targeting molecules.[34, 43] In this study, we construct a highly swollen polyelectrolyte multilayer for IOL material modification, taking advantages of the highly hydrated state of the polysaccharide HA and CHI. With the water content as high as 400% after 5 bilayer deposition, (HA/CHI)$_5$ multilayer modified IOL materials show excellent cell resistant property, not only in vitro, but also in vivo. Although such multilayer modified IOL doesn't reduce the Soemmerring ring formation and the PPCO occurrence, the

CPCO incidence is greatly reduced. As reduced LEC adhesion may be result in reduced cell proliferation and migration, the hydrated polysaccharide multilayer modification of the IOL shows positive effects on the PCO prevention and may prolong the clinically service life of the IOL.
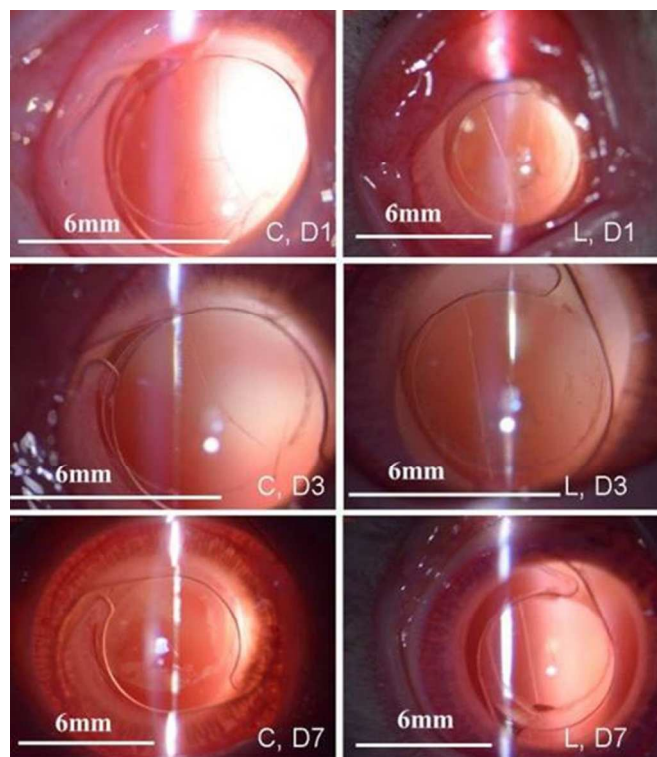

Fig. 12 Slit lamp micrographs of IOL with (L) or without (C) (HA/CHI)$_5$ multilayer modification in rabbit eye.
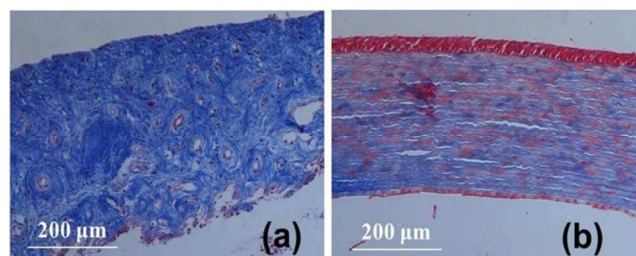

Fig. 13 Light photomicrographs of histopathological sections of iris (a) and cornea (b) cut from (HA/CHI)$_5$ multilayer modified IOL implanted eye of rabbits. Masson trichrome staining, original magnification is ×200.
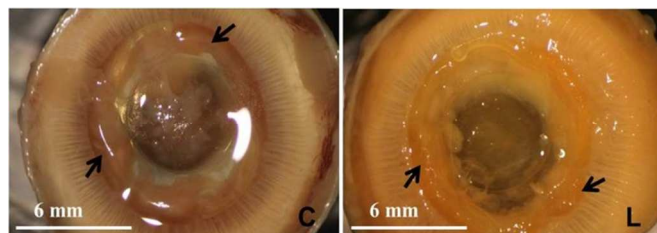

Fig. 14 Gross photographs (Miyake-Apple view) of IOL implanted rabbit eyes. C: pristine IOL (control IOL) with diffuse PCO. L: (HA/CHI)$_5$ multilayer modified IOL (study IOL) showing overall clear anterior and posterior capsules. The arrows delineate the localized area where Soemmerring ring formation was observed in this eye.
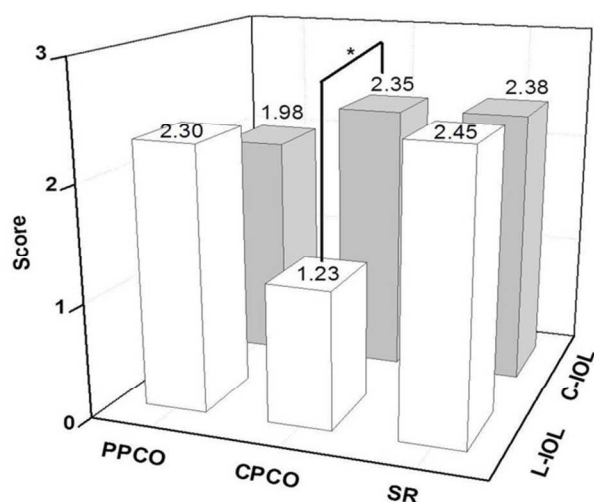
Fig. 15 Peripheral PCO (PPCO), Central PCO (CPCO) and Soemmerring Ring (SR) scores of control IOL (C-IOL) and $(HA/CHI)_5$ multilayer modified IOL (L-IOL).

Conclusions

Polysaccharide multilayer was successfully introduced onto hydrophobic silicone IOL. Taking advantages of the high hydration of the natural polysaccharide multilayer, the fabricated multilayer coating takes on excellent swollen property. The water content is as high as 400% when 5 bialyer of HA and CHI multilayer was constructed. Although the decrease of protein adsorption is not notable, the in vitro LEC adhesion and proliferation are distinctly reduced. The in vivo implantation of the IOL with swollen polysaccharide multilayer modification shows reduced residue LEC and cortex adhesion in vivo. Reduced CPCO incidence is found on such multilayer modified IOL cases. These results demonstrate that such swollen polysaccharide multilayer may be a good alternative for IOL surface modification for anti-PCO application.

Acknowledgements

Notes and references

[a] School of Ophthalmology & Optometry, Eye Hospital, Wenzhou Medical University, Wenzhou 325027, China

[b] Wenzhou Institute of Biomaterials and Engineering, Wenzhou, 32500, China

* Corresponding author. Fax: +86 577 88067962.

E-mail: lqk97531@126.com (Q.K. Lin), Chenhao823@mail.eye.ac.cn (H. Chen),

1. R. Stanic, K. Bucan, K. Stanic-Jurasin and Z. Kovacic, *Acta Clin. Croat.*, 2012, **51**, 55-58.

2. I. M. Wormstone, L. Wang and C. S. C. Liu, *J. Cataract Refr. Surg.*, 2009, **88**, 257-269.

3. X. L. Liu, B. Cheng, D. Y. Zheng, Y. H. Liu and Y. Z. Liu, *J. Cataract Refr. Surg.*, 2010, **36**, 208-214.

4. S. Saika, *Prog. Retin. Eye Res.*, 2004, **23**, 283-305.

5. L. Werner, *Curr. Opin. Ophthalmol.*, 2008, **19**, 41-49.

6. H. Matsushima, H. Iwamoto, K. Mukai, Y. Katsuki, M. Nagata and T. Senoo, *Expert Rev. Med. Devic.*, 2008, **5**, 197-207.

7. C. B. Sun, W. Q. Teng, J. T. Cui, X. J. Huang and K. Yao, *Colloid. Surface. B*, 2014, **113**, 33-42.

8. N. Awasthi, S. T. Wang-Su and B. J. Wagner, *Invest. Ophth. Vis. Sci.*, 2008, **49**, 1998-2003.

9. R. Alon, E. I. Assia and G. Kleinmann, *Invest. Ophth. Vis. Sci.*, 2014, **55**, 4005-4013.

10. B. Amoozgar, D. Morarescu and H. Sheardown, *Colloid. Surface. B*, 2013, **111**, 15-23.

11. D. Bozukova, C. Pagnoulle, M. C. De Pauw-Gillet, S. Desbief, R. Lazzaroni, N. Ruth, R. Jerome and C. Jerome, *Biomacromolecules*, 2007, **8**, 2379-2387.

12. D. J. Li, F. Z. Cui and H. Q. Gu, *Biomaterials*, 1999, **20**, 1889-1896.

13. C. Abela-Formanek, M. Amon, G. Kahraman, J. Schauersberger and R. Dunavoelgyi, *J. Cataract Refr. Surg.*, 2011, **37**, 104-112.

14. K. Yao, X. D. Huang, X. J. Huang and Z. K. Xu, *J. Biomed. Mater. Res. A*, 2006, **78A**, 684-692.

15. D. Bozukova, C. Pagnoulle, R. Jerome and C. Jerome, *Mat. Sci. Eng. R*, 2010, **69**, 63-83.

16. B. L. Wang, Q. K. Lin, C. H. Shen, Y. M. Han, J. M Tang and H. Chen, *Rsc Adv.*, 2014, **4**, 52959-52966.

17. B. L. Wang, Q. K. Lin, C. H. Shen, J. M. Tang, Y. M. Han and H. Chen, *J. Colloid Interf. Sci.*, 2014, **431**, 1-7.

18. C. P. McCoy, R. A. Craig, S. M. McGlinchey, L. Carson, D. S. Jones and S. P. Gorman, *Biomaterials*, 2012, **33**, 7952-7958.

19. F. Parra, B. Vazquez, L. Benito, J. Barcenilla and J. San Roman, *Biomacromolecules*, 2009, **10**, 3055-3061.

20. P. Yammine, G. Pavon-Djavid, G. Helary and V. Migonney, *Biomacromolecules*, 2005, **6**, 2630-2637.

21. B. Amoozgar, S. D. Fitzpatrick and H. Sheardown, *Journal of J. Bioact. Compat. Pol.*, 2013, **28**, 637-651.

22. M. K. Kim, I. S. Park, H. D. Park, W. R. Wee, J. H. Lee, K. D. Park, S. H. Kim and Y. H. Kim, *J. Cataract Refr. Surg.*, 2001, **27**, 766-774.

23. Z. W. Zheng, K. M. Deng, L. Ren and Y. J. Wang, *Chem. J. Chinese U.*, 2012, **33**, 1350-1354.

24. A. Kobayashi, A. Ando, N. Tagami, M. Kitagawa, E. Kawai, M. Akioka, E. Arai, T. Nakatani, S. Nakano, Y. Matsui and M. Matsumura, *J. Ocul. Pharmacol. Th.*, 2008, **24**, 607-612.

25. R. R. Costa and J. F. Mano, *Chem. Soc. Rev.*, 2014, **43**, 3453-3479.

26. V. Gribova, R. Auzely-Velty and C. Picart, *Chem. Mater.*, 2012, **24**, 854-869.

27. C. Picart, *Curr. Med. Chem.*, 2008, **15**, 685-697.

28. S. Hossfeld, A. Nolte, H. Hartmann, M. Recke, M. Schaller, T. Walker, J. Kjems, B. Schlosshauer, D. Stoll, H. P. Wendel and R. Krastev, *Acta Biomater.*, 2013, **9**, 6741-6752.

29. S. L. Bechler, Y. Si, Y. Yu, J. Ren, B. Liu and D. M. Lynn, *Biomaterials*, 2013, **34**, 226-236.

30. Q. K. Lin, X. Ding, F. Y. Qiu, X. X. Song, G. S. Fu and J. Ji, *Biomaterials*, 2010, **31**, 4017-4025.

31. S. Meng, Z. J. Liu, L. Shen, Z. Guo, L. L. Chou, W. Zhong, Q. G. Du and J. B. Ge, *Biomaterials*, 2009, **30**, 2276-2283.

32. Q. K. Lin, J. J. Yan, J. Ji and J. C. Shen, *Chem. J. Chinese U.*, 2009, **30**, 1256-1258.

33. Q. K. Lin, J. J. Yan, F. Y. Qiu, X. X. Song, G. S. Fu and J. Ji, *J. Biomed. Mater. Res. A*, 2011, **96A**, 132-141.

34. Q. K. Lin, Y. Hou, X. Xu, J. Tang, Y. Han, H. Chen and J. Ji, *Int. J. Polym. Mater.*, 2015, **64**, 99-103.

35. Y. X. Sun, K. F. Ren, J. L. Wan, G. X. Chang and J. Ji, *ACS Appl. Mater. Interf.*, 2013, **5**, 4597-4602.

36. W. Qi, P. Cai, W. J. Yuan and H. Wang, *J. Biomed. Mater. Res. A*, 2014, **102**, 4071-4077.

37. X. D. Huang, K. Yao, Z. Zhang, Y. Zhang and Y. Wang, *J. Cataract Refr. Surg.*, 2010, **36**, 290-298.

38. J. Necas, L. Bartosikova, P. Brauner and J. Kolar, *Vet. Med.-CZECH*, 2008, **53**, 397-411.

39. I. S. Barequet, N. Harizman, H. Ziv and M. Rosner, *Cornea*, 2014, **33**, 1080-1082.

40. W. T. Ho, T. H. Chiang, S.W. Chang, Y. H. Chen, F. R. Hu and I. J. Wang, *Clin. Exp. Optom.*, 2013, **96**, 536-541.

41. M. Kumar, *React. Funct. Polym.*, 2000, **46**, 1-27.

42. Y. Hou, Q. K. Lin, J. Ji and J. C. Shen, *Chem. J. Chinese U.*, 2008, **29**, 1890-1894.

43. Q. K. Lin, Y. Hou, K. F. Ren and J. Ji, *Thin Solid Films*, 2012, **520**, 4971-4978.

44. Q. K. Lin, K. F. Ren and J. Ji, *Colloid. Surface. B*, 2009, **74**, 298-303.

45. F. Croisier, G. Atanasova, Y. Poumay and C. Jerome, *Adv. Healthc. Mater.*, 2014, **3**, 2032-2039.

46. J. M. Silva, A. R. C. Duarte, S. G. Caridade, C. Picart, R. L. Reis and J. F. Mano, *Biomacromolecules*, 2014, **15**, 3817-3826.

47. G. M. Liu, J. P. Zhao, Q. Y. Sun and G. Z. Zhang, *J. Phys. Chem. B*, 2008, **112**, 3333-3338.

48. L. Richert, P. Lavalle, E. Payan, X. Z. Shu, G. D. Prestwich, J. F. Stoltz, P. Schaaf, J. C. Voegel and C. Picart, *Langmuir*, 2004, **20**, 448-458.

49. A. C. Schroeder, C. Lingenfelder, B. Seitz, U. Grabowy, C. W. Spraul, Z. Gatzioufas and M. Herrmann, *Graef. Arch. Clin. Exp.*, 2009, **247**, 1277-1283.

50. L. Richert, Y. Arntz, P. Schaaf, J. C. Voegel and C. Picart, *Surf. Sci.*, 2004, **570**, 13-29.

51. A. Schneider, G. Francius, R. Obeid, P. Schwinte, J. Hemmerle, B. Frisch, P. Schaaf, J. C. Voegel, B. Senger and C. Picart, *Langmuir*, 2006, **22**, 1193-1200.

52. D. L. Elbert, C. B. Herbert and J. A. Hubbell, *Langmuir*, 1999, **15**, 5355-5362.

53. G. K. Klintworth, *Am. J. Pathol.*, 1977, **89**, 718-808.

54. J. D. Mendelsohn, S. Y. Yang, J. Hiller, A. I. Hochbaum and M. F. Rubner. *Biomacromolecules*, 2003, **4**, 96–106.
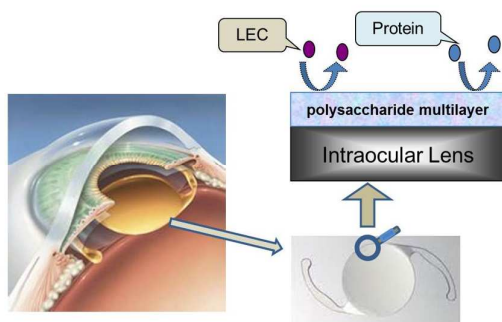
Swollen polysaccharide multilayer was coated on IOL for inhibiting LEC adhesion and proliferation, thus decrease the PCO incidence after implantation.